# Computational Fluid Dynamic (CFD) Simulation of Ultrahigh Velocity Abrasive Waterjet

**Author/Contributor:**
Liu, H.; Wang, Jun; Brown, R.J.; Kelson, N.

**Publication details:**
Key Engineering Materials
v. 233-236
pp. 477-482

**Publication Date:**
2003

Key Engineering Materials, Vols. 233-236 (2003), 477-482.

# Computational Fluid Dynamic (CFD) Simulation of Ultrahigh Velocity Abrasive Waterjet

H. Liu[1], J. Wang[1,*], R.J. Brown[1] and N. Kelson[2]

[1] School of Mechanical, Manufacturing & Medical Engineering, Queensland University of Technology, GPO Box 2434, Brisbane, Qld 4001, Australia

[2] Information Technology Services, Queensland University of Technology, Australia

**Keywords**: Abrasive waterjet, Computational fluid dynamics, Multiphase axisymmetric flow

**Abstract.** A computational fluid dynamic (CFD) model for the ultrahigh velocity abrasive waterjet (AWJ) is established using a commercial CFD package, Fluent5. The model is then used to simulate the jet dynamic characteristics after it flows through a fine nozzle under the steady state, turbulent, and three-phase flow conditions. The selection of boundary conditions, initial guess, solver control, and convergence strategies of the model is discussed. Plausible characteristics of the flow as well as the particle velocity and trajectory at different input conditions are predicted and discussed. It is shown that within the computational domain of 10 mm considered, there is a minimum variation of the velocity and pressure along the jet while the variation across the jet is not significant within 80% of the jet diameter. Interpretations of some cutting phenomena in AWJ cutting based on these findings are also given.

## Introduction

Abrasive waterjet (AWJ) cutting is one of the most recently developed non-traditional cutting processes. Comparing with the traditional and other non-traditional machining methods, AWJ cutting technology has its various distinct advantages, such as no thermal distortion, high machining versatility, ability to produce contours, good surface quality, easy integration with mechanical manipulators, and minimal burr [1]. Consequently, AWJ cutting has found extensive application in manufacture industry for machining a wide range of metals and nonmetals [2]. It has been particularly used in cutting 'difficult-to-cut' materials such as ceramics and marbles [3-5], and layered composites [6-8] as well as in pattern cutting on various materials.

Abrasive water jet technology uses a fine jet of ultrahigh pressure water and abrasive slurry to cut the target material by means of erosion. Since the introduction of AWJ cutting technology, a large amount of research and development effort has been made to explore its applications and associated science [2]. However, this technology is still under flux and development and its many aspects remain to be fully understood. In addition, very little reported research has been directed towards achieving a fundamental understanding of the dynamic behaviour of abrasive water jet such as the distribution of velocity and pressure in the jet [9, 10]. This has limited the development of this cutting technology. An understanding of the dynamic characteristics of an abrasive waterjet is essential for improving the nozzle design, improving the cutting performance as well as modelling and evaluating the jet cutting performance.

The present work is attempted to gain a fundamental understanding of the jet dynamic characteristics with a view to provide a theoretical basis for enhancing the AWJ cutting technology and modeling the various cutting performance measures that are required for effective process control in practice. For this purpose, Computational fluid dynamic (CFD) analysis is found to be convenient because direct measurement of particle velocities and visualization of particle trajectories are very difficult for the ultrahigh speed and small dimensions. Specifically, this paper

* Corresponding Author. Fax: (07) 3864 1469, Email: j.wang@qut.edu.au.

reports on a preliminary study of the ultrahigh velocity abrasive waterjet after it comes through a very fine nozzle. The CFD model is established based on three-phase (air, water and particle) turbulent flow. Using this model the abrasive particle velocity and trajectories are calculated, and the distribution of velocity and pressure in the jet is also presented and discussed.

## Model Formulation

For the purpose of this work that is to predict the distribution of velocity and pressure in the abrasive waterjet and the particle dynamic properties, the CFD simulation is performed with the FLUENT5.5 package. The governing equations and the boundary conditions for this stimulation study are given below.

**Governing equations**. The multiphase volume of fluid (VOF) model available in Fluent is chosen to simulate the water flow. Initially, the CFD model considers the two-phase (air and water) flow, where air is treated as primary phase. In Cartesian tensors, the relevant equations are given below.

The continuity equation for the volume fraction of qth phase is:

$$\frac{\partial \alpha_q}{\partial t} + u_i \frac{\partial \alpha_q}{\partial x_i} = 0 \tag{1}$$

where $\alpha_q$ donates the qth phase volume fraction. The volume fraction equation is not solved for the primary phase; the primary-phase volume fraction is computed based on the constraint that the sum of volume fraction of all phases is one.

The momentum equation is solved throughout the domain, and the resulting velocity field is shared among the phases:

$$\frac{\partial}{\partial t}\rho u_j + \frac{\partial}{\partial x_i}\rho u_i u_j = -\frac{\partial P}{\partial x_j} + \frac{\partial}{\partial x_i}\mu\left(\frac{\partial u_i}{\partial x_j} + \frac{\partial u_j}{\partial x_i}\right) + \frac{\partial}{\partial x_j}\left(-\rho\overline{u_i' u_j'}\right) \tag{2}$$

Transport equations for the turbulence energy *k* and dissipation rate ε are solved, and shared by the phases throughout the field. The standard k-ε model is chosen in this simulation work. This model is mathematically given by:

$$\rho\frac{Dk}{Dt} = \frac{\partial}{\partial x_i}\left[\left(\mu + \frac{\mu_t}{\sigma_k}\right)\frac{\partial k}{\partial x_i}\right] + G_k - \rho\varepsilon \tag{3}$$

and

$$\rho\frac{D\varepsilon}{Dt} = \frac{\partial}{\partial x_i}\left[\left(\mu + \frac{\mu_t}{\sigma_\varepsilon}\right)\frac{\partial \varepsilon}{\partial x_i}\right] + C_{1\varepsilon}\frac{\varepsilon}{k}G_k - C_{2\varepsilon}\rho\frac{\varepsilon^2}{k} \tag{4}$$

where $\mu_t = \rho C_\mu \frac{k^2}{\varepsilon}$ is the turbulent viscosity and $G_k$ is the generation of turbulent kinetic energy due to the mean velocity gradients. $C_\mu = 0.09$, $C_{1\varepsilon} = 1.44$, $C_{2\varepsilon} = 1.92$, $\sigma_k = 1$ and $\sigma_\varepsilon = 1.3$ are the usual values for the standard k-ε model.

The effect of the particles on the continuum is neglected in this study as are the particle-particle interactions. Fluent calculates the particle trajectories by integrating the force balance on each particle which includes the particle inertia and drag force, and for a single particle, the force balance equation can be written as:

$$\frac{du_p}{dt} = F_D(u - u_p) \tag{5}$$

where $F_D(u-u_p)$ is the drag force per unit particle mass and $F_D = \frac{18\mu}{\rho_p D_p^{\,2}} \frac{C_D R_e}{24}$, u is the fluid phase velocity, $u_p$ is the particle velocity, μ is the molecular viscosity of the fluid (i.e. water in this study), ρ is the fluid density, $\rho_p$ is the density of particle (garnet is used in this study), $D_p$ is the particle diameter, $R_e$ is relative Reynolds number, and $C_D$ is the drag coefficient.

These general governing equations are then converted into their polar coordinate forms and used for steady state, turbulent, incompressible, two-phase axisymmetric flow. A control-volume-based technique is used to convert the governing equations to algebraic equations that can be solved numerically. After the solution of pure water jet has been achieved, particle motions and trajectories were solved by using Discrete Phase Modelling available in Fluent.

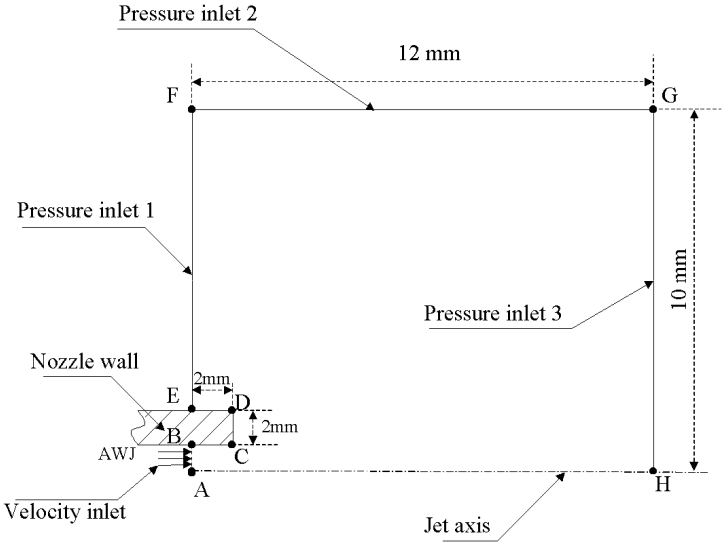


Fig. 1. Geometry and boundary conditions of the CFD computational domain.

**Assumptions and Boundary conditions**. Fig. 1 shows the geometry of the computational domain with boundary conditions. The fluid flow field is solved first. A pure water jet is considered as a two-dimensional, steady axisymmetric turbulent flow that passes through a thin nozzle of 1 mm in diameter and enters the atmosphere as a free jet. In the CFD model, the jet enters the computational domain across section AB as shown in Fig. 1 with the velocity varying up to 950m/s. In this simulation, the water velocity across the jet before flowing out of the nozzle is assumed to have two types of distributions, i.e. uniformly distributed and the 1/7 power law distribution [11] with the maximum value of 950m/s. These velocity inlet conditions were applied across AB along with the default solver values for the turbulent kinetic energy and dissipation rate. In addition, the liquid volume fraction is set to one over this boundary.

After a viable and accurate solution is obtained, abrasive particles are added into the pure water jet across the inlet while attention is paid to only one particle and assuming that there is no interference between particles. It is also assumed that the initial particle velocity at the inlet is the same as the velocity of its surrounding water. Based on these conditions, the particle velocities and trajectories are calculated. Fluent5 is capable of free surface flow computations and has Lagrangian particle tracking with momentum coupling to the flow-field feature.

In the CFD model, sections EF, FG and GH of Fig. 1 are considered as free boundaries and the pressure inlet conditions are used for these boundaries. Also, it is expected that only air will be entrained into the computational domain; therefore, the air volume fraction for any fluid *entering* the domain across EF, FG or GH is set to one.

## Results and Discussion

**Dynamic Characteristics of the Water Flow Field**. The velocity and pressure distribution along the jet axial direction is analysed first. Some representative results are shown in Fig. 2 where the axial distance is originated at the velocity inlet, i.e. the cross-section AB. It can be seen that along the centre-line of the jet, the magnitude of the velocity increases initially, then stabilizes within the computational domain. It is further noticed that the velocity increasing segment corresponds to the flow within the nozzle. The increase of the velocity in the jet centre within the nozzle region is believed to be a result of the conservation of mass in the incompressible flow where the velocity in the jet outer rim may decrease slightly. The relatively constant velocity in the rest of the domain is consistent with the early studies [12,13]. It seems that the computational domain in this study falls in the "initial region" where the dynamic pressure, and hence velocity, variation is minimum. While the current study can accommodate most of the practical cases, further study is needed to extend the computational domain. This result has confirmed that the stand-off distance between the nozzle and workpiece in AWJ cutting in the practical range of 2 and 5 mm has no significant effect on the cutting performance.

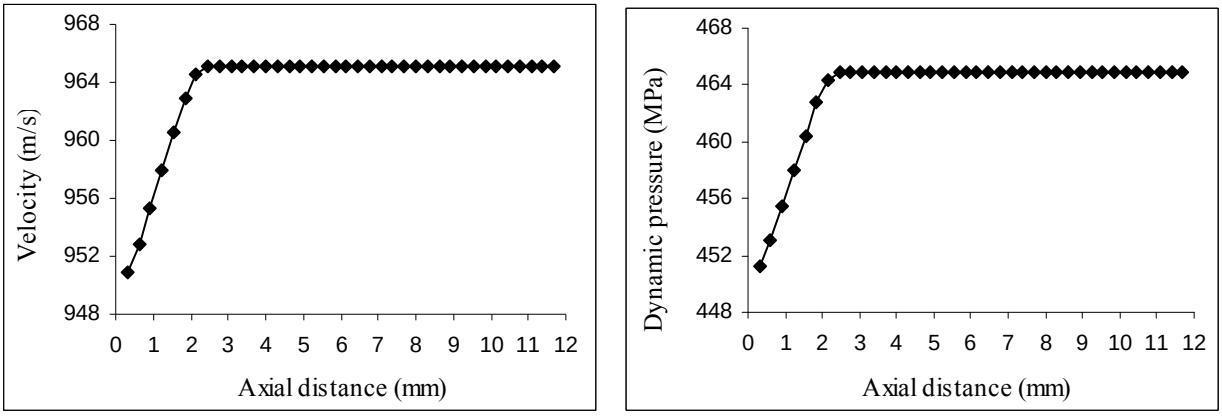


(a) (b)

Fig. 2. Velocity magnitude and dynamic pressure of water jet along the centre line.

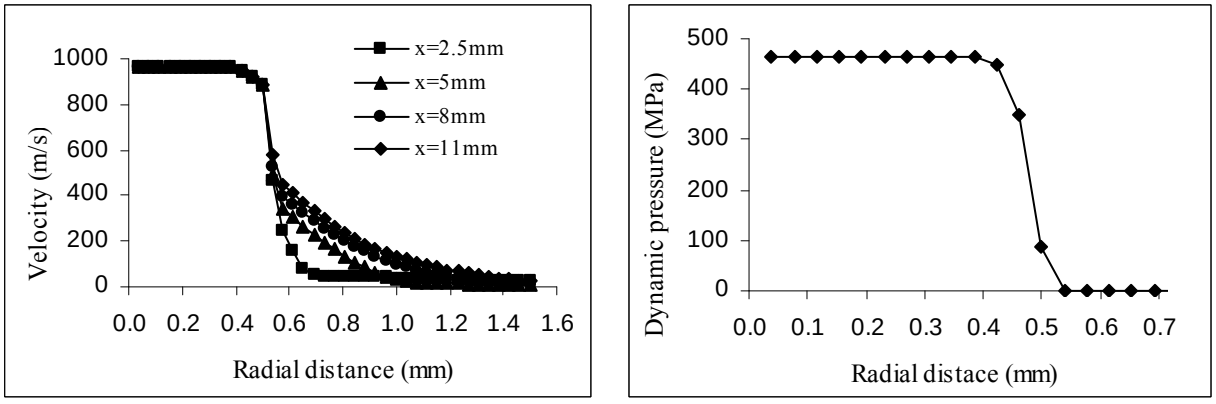


(a) (b)

Fig. 3. Radial profile of velocity and dynamic pressure.

Fig. 3 shows the profile of velocity and dynamic pressure in the radial direction. In Fig. 3(a), four cross-sections at 2.5 mm, 5 mm, 8 mm and 11 mm from the origin (AB) are considered to illustrate the velocity distribution in the jet radial direction. It can be seen that when the radial distance from the jet core is within 0.5 mm, there is no discernible difference between the velocities at the four cross sections, this being consistent with the finding above along the jet axial direction. However, as the radial distance from the jet centre increases the water velocity decreases which

follows somehow an exponential curve. This is particularly evident when the radial distance is greater than 0.4 mm. A further increase in the radial distance will go beyond the jet domain where the air interacting with the water has gained velocity. This velocity will subsequently decrease as the radial distance is increased.

The dynamic pressure profiles of free jet at all cross sections do not exhibit discernible difference. As shown in Figure 3, the dynamic pressure decreases slightly near the free surface of the jet and then decreases abruptly to zero. The study of water jet profile from the computed solution indicates that the jet does not spread significantly, but maintains a nearly constant diameter throughout the computational domain. This is primarily because of the short computational domain considered in this study and is again consistent with the earlier studies [12,13]. This finding implies that for the relatively short standoff distance used in AWJ cutting, the effect of standoff on the top kerf width is minimal.

**Particle Velocity and Trajectory**.

The particles were assumed to be spherical and the CFD study used garnet particles of three different particle sizes or diameters, i.e. 0.1mm, 0.02 mm and 0.18mm. The particles were injected into the flow across the inlet AB with the same velocity as the water jet.

Fig. 4 shows the particle velocity distributions in the abrasive water jet together with the water velocity for comparison purpose. The particle velocity along the jet centre-line is presented in Fig. 4(a). It appears that inside the abrasive water jet, the particles are accelerated with the water. The particles do not have the same velocity as the water because of their heaver density and larger inertia. Different sizes of particles appear to have different behavours in the jet. It seems that small particles can gain more acceleration and hence higher speed which approaches the water speed after traveling some distance from the nozzle. By contrast, large particles exhibit relative stable travel velocity in the water.

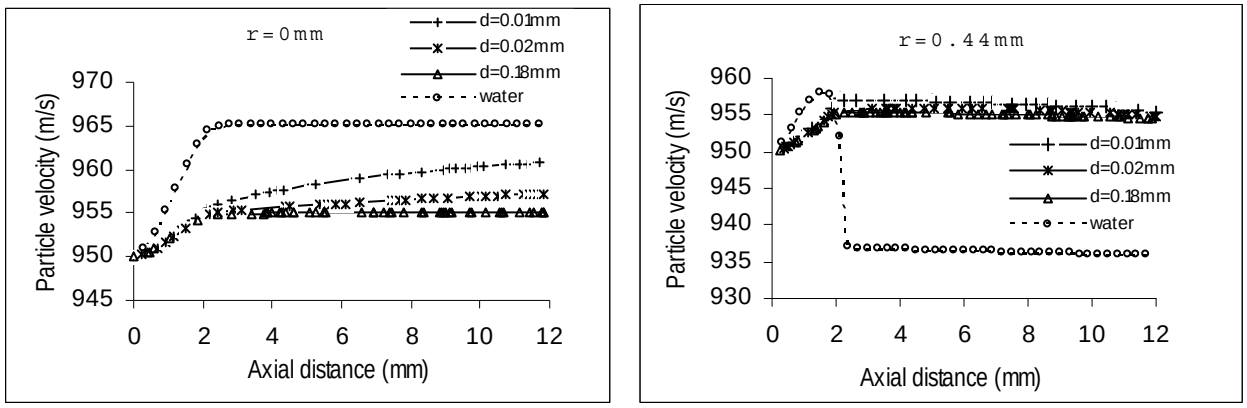


(a) (b)

Fig. 4. Particle velocity distribution along the axial direction at different radial distances.

Fig. 4 (b) demonstrates the velocity of particles that were injected into the water jet at 0.44 mm away from the jet core (r=0.44 mm). As mentioned earlier, because of the interaction between the water and air after the jet flows out of the nozzle, the water velocity in this region is decreased as the jet travels away from the nozzle. As a result, the velocity of the particles in this region also decreases. However, it appears that the particle inertia can maintain the particle to travel at relatively stable speed that is higher than the surrounding water speed. For the three particle sizes considered in this study, the influence of particle size on the particle velocity in this region is not significant.

In addition, each type of particles was released into the waterjet at the locations of different distances from the jet core to investigate the particle trajectory. The results show that particle size

and injecting location have no influence on the particle trajectory, and the particles follow a continuous flow motion.

## Conclusions

A CFD simulation study on the dynamic characteristics of the water jet and abrasive water jet has been presented. The preliminary study has provided a better understanding of the dynamic features of the jet and particles which are often difficult to investigate by other means. Based on this study, there is a minimum variation of the water pressure and velocity within the computational domain in the jet axial direction, which suggests that the cutting performance is relatively independent of standoff distance for the typical standoff distance used in AWJ cutting. It has also shown that the velocity and pressure variation in the radial direction is not significant within about 80% to 90% of the jet diameter. This finding has formed the basis to estimate the top kerf width from the knowledge of the jet or nozzle diameter. In addition, it has been shown that CFD simulation can provide the information of particle velocities and trajectories which make it possible to determine the particle impact angle as well as the impinging speed and location.

Future work is being carried out to study the jet and particle characteristics within the nozzle and the jet and using extended domain and boundary conditions. It is hoped that this study will be able to optimize the nozzle design and arrive at mathematical models for these characteristics for use in modeling the cutting performance in AWJ machining.

## References


[1] C.A. van Luttervelt: On the selection of manufacturing methods illustrated by an overview of separation techniques for sheet materials. *Annals of CIRP*, Vol. 38 (1989), pp. 587-607.

[2] A.W. Momber: Principles of abrasive waterjet machining (Springer-Verlag, London 1998).

[3] J. Zeng and T.J. Kim: An erosion model of polycrystalline ceramics in abrasive waterjet cutting. *Wear*, Vol. 193 (1996), pp. 207-217.

[4] H. Hocheng and K.R. Chang: Material removal analysis in abrasive waterjet cutting of ceramic plate. *J. Mater. Proc. Technol*. Vol. 40 (1994), pp. 287-304.

[5] G.V.S. Prasad, J. Wang and W.C.K. Wong: Kerf formation analysis in the abrasive waterjet machining of industrial Ceramics, *Advances in Abrasive Technology* II (Japan Society of Grinding Engineers 1998), pp. 213-220.

[6] E. Capello, M. Monno, Q. Semeraro and P. di Milano: Delamination in water jet cutting of multi-layered composite material. *Proc. 12th Conf. Jet Cutting Technol*. (1994), pp.463-476

[7] J. Wang: Abrasive waterjet machining of polymer matrix composites: Cutting performance, erosive analysis and predictive models. *Int. J. Adv. Manuf. Technol*., Vol. 15 (1999), pp. 757-768.

[8] J. Wang: A predictive depth of penetration model for abrasive waterjet cutting of polymer matrix composites. *J. Mater. Proc. Technol*.. Vol. 121/2-3 (2002), pp. 390-394.

[9] J. Ye, R. Kovacevic: Turbulent solid-liquid flow through the nozzle of premixed abrasive waterjet. Proc. Inst. Mech. Engrs., Part B, Vol. 213 (1999), pp. 59-67

[10] H.T. Liu and P. Miles: CFD and physical modelling of UHP AWJ drilling. *Proc. 14th Int. Conf. Jetting Technol*. (Belgium 1998), pp. 15-24.

[11] V.L. Streeter, E.F. Wylie and K.W. Bedford: *Fluid Mechanics* (WCB/McGraw Hill 1998)

[12] K.Yanaida: Flow characteristics of water Jets. *Proc. Symp. Jet Cutting* (1974), pp. 20-32

[13] M. Hashish and M.P. du Plessis: Prediction equations relating high velocity jet cutting performance to stand off distance and multipasses. *J. Eng. Ind.*, Vol. 101 (1979), pp. 311-319.